

Mycobacteria as a public health risk - Discussion

Re: Haghkhah 2012-10-08 Search results

Web of Science®

Topic=(mycobacter* AND "image analysis")

Timespan=All Years

Databases=SCI-EXPANDED, SSCI, A&HCI, CPCI-S, CPCI-SSH, CCR-EXPANDED, IC

Lemmatization=On

Results: 45

Searched on 2012-10-08 by K. Hruska

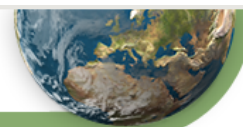
Refined by: Topic=(paratub*): 2 (records 31 and 43)

- 1 Saha, R., Donofrio, R.S., Goeres, D.M., Bagley, S.T. (2012)
Rapid detection of rRNA group I pseudomonads in contaminated metalworking fluids and biofilm formation by fluorescent in situ hybridization
Applied Microbiology and Biotechnology, 94, 799-808

Metalworking fluids (MWFs), used in different machining operations, are highly prone to microbial degradation. Microbial communities present in MWFs lead to biofilm formation in the MWF systems, which act as a continuous source of contamination. Species of rRNA group I *Pseudomonas* dominate in contaminated MWFs. However, their actual distribution is typically underestimated when using standard culturing techniques as most fail to grow on the commonly used *Pseudomonas* Isolation Agar. To overcome this, fluorescent in situ hybridization (FISH) was used to study their abundance along with biofilm formation by two species recovered from MWFs, *Pseudomonas fluorescens* MWF-1 and the newly described *Pseudomonas oleovorans* subsp. *lubrificantis*. Based on 16S rRNA sequences, a unique fluorescent molecular probe (Pseudo120) was designed targeting a conserved signature sequence common to all rRNA group I *Pseudomonas*. The specificity of the probe was evaluated using hybridization experiments with whole cells of different *Pseudomonas* species. The probe's sensitivity was determined to be 10^3 cells/ml. It successfully detected and enumerated the abundance and distribution of *Pseudomonas* indicating levels between $3.2 (+/- 1.1) \times 10^6$ and $5.0 (+/- 2.3) \times 10^6$ cells/ml in four different industrial MWF samples collected from three different locations. Biofilm formation was visualized under stagnant conditions using high and low concentrations of cells for both *P. fluorescens* MWF-1 and *P. oleovorans* subsp. *lubrificantis* stained with methylene blue and Pseudo120. On the basis of these observations, this molecular probe can be successfully used in the management of MWF systems to monitor the levels and biofilm formation of rRNA group I pseudomonads

- 2 Rahman, S., Magalhaes, I., Rahman, J., Ahmed, R.K., Sizemore, D.R., Scanga, C.A., Weichold, F., Verreck, F., Kondova, I., Sadoff, J., Thorstensson, R., Spangberg, M., Svensson, M., Andersson, J., Maeurer, M., Brighenti, S. (2012)
Prime-Boost Vaccination with rBCG/rAd35 Enhances CD8(+) Cytolytic T-Cell Responses in Lesions from Mycobacterium Tuberculosis-Infected Primates
Molecular Medicine, 18, 647-658

To prevent the global spread of tuberculosis (TB) infection, a novel vaccine that triggers potent and long-lived immunity is urgently required. A plasmid-based vaccine has been developed to enhance activation of major histocompatibility complex (MHC) class I-restricted CD8+ cytolytic T cells using a recombinant *Bacille Calmette-Guerin* (rBCG) expressing a pore-forming toxin and the *Mycobacterium tuberculosis* (Mtb) antigens Ag85A, 85B and TB10.4 followed by a booster with a nonreplicating adenovirus 35 (rAd35) vaccine vector encoding the same Mtb antigens. Here, the capacity of the rBCG/rAd35 vaccine to induce protective and biologically relevant CD8(+) T-cell responses in a nonhuman primate model of TB was investigated. After prime/boost immunizations and challenge with virulent Mtb in rhesus macaques, quantification of immune responses at the single-cell level in cryopreserved tissue specimen from infected organs was performed using in situ computerized image analysis as a technological platform. Significantly elevated levels of CD3(+) and CD8(+) T cells as well as cells expressing interleukin (IL)-7, perforin and granulysin were found in TB lung lesions and spleen from rBCG/rAd35-vaccinated animals compared with BCG/rAd35-vaccinated or unvaccinated animals. The local increase in CD8(+) cytolytic T cells correlated with reduced expression of the Mtb antigen MPT64 and also with prolonged survival after the challenge. Our observations suggest that a protective immune response in rBCG/rAd35-vaccinated nonhuman primates was associated with enhanced MHC class I antigen presentation and activation of CD8+ effector T-cell responses at the local site of infection in Mtb-challenged animals. Online address: <http://www.molmed.org> doi: 10.2119/molmed.2011.00222



- 3 Delaby, A., Espinosa, L., Lepolard, C., Capo, C., Mege, J.L. (2010)
3D reconstruction of granulomas from transmitted light images implemented for long-time microscope applications
Journal of Immunological Methods, 360, 10-19

Image analysis tools are essential to describe and quantify dynamic biological phenomena, such as early stages of granuloma formation. Granulomas are constituted of a collection of immune cells that contain pathogens. leading to their elimination. We presented here a new method to obtain granuloma 3D reconstruction from transmitted light images. Granulomas were generated by incubating peripheral blood mononuclear cells with beads coated with sonicated *Coxiella burnetii*, a bacterial pathogen. Biological samples were observed under a confocal microscope, and recorded during several hours, providing a large set of data of several gigabytes. Our image processing, called Focus Detection Plugin (FDP), allowed to extract relevant images from large datasets and to perform a deblurring of image stacks. This FDP method, that was implemented as an ImageJ plugin, did not require powerful computer resources and was simple to use. To validate our FDP method, we compared our results with 3D reconstruction of fluorescent images. Both methods yielded comparable results. We concluded that our FDP method was able to generate processed images yielding robust 3D reconstruction of whole cell bodies, and presented major advantages for long-time recordings since no cell labeling was needed. This method was convenient to study the early stages of granuloma formation and may be applied to other complex biological systems. (C) 2010 Elsevier B.V. All rights reserved

- 4 Christophe, T., Ewann, F., Jeon, H.K., Cechetto, J., Brodin, P. (2010)
High-content imaging of Mycobacterium tuberculosis-infected macrophages: an in vitro model for tuberculosis drug discovery
Future Medicinal Chemistry, 2, 1283-1293

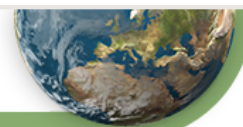
Macrophages are reservoirs for replicating mycobacterium during tuberculosis (TB) infections. In this study, small molecules to be developed as anti-tubercular treatments were investigated for their ability to kill intracellular bacteria in in vitro macrophage models. High-content imaging technologies offer a high-throughput method to quantify a drug's ability to inhibit Mycobacterium tuberculosis intracellular invasion and multiplication in host cells. Dedicated image analysis enables the automated quantification of infected macrophages, and compounds that inhibit mycobacteria proliferation can be tested using this method. Furthermore, the implementation of the assay in 384-well microtiter plates combined with automated image acquisition and analysis allows large-scale screening of compound libraries in M. tuberculosis-infected macrophages. Here we describe a high-throughput and high-content workflow and detail its utility for the development of new TB drugs

- 5 den Hertog, A.L., Visser, D.W., Ingham, C.J., Fey, F.H.A.G., Klatser, P.R., Anthony, R.M. (2010)
Simplified Automated Image Analysis for Detection and Phenotyping of Mycobacterium tuberculosis on Porous Supports by Monitoring Growing Microcolonies

Plos One, 5, Background: Even with the advent of nucleic acid (NA) amplification technologies the culture of mycobacteria for diagnostic and other applications remains of critical importance. Notably microscopic observed drug susceptibility testing (MODS), as opposed to traditional culture on solid media or automated liquid culture, has shown potential to both speed up and increase the provision of mycobacterial culture in high burden settings. Methods: Here we explore the growth of Mycobacterial tuberculosis microcolonies, imaged by automated digital microscopy, cultured on a porous aluminium oxide (PAO) supports. Repeated imaging during colony growth greatly simplifies "computer vision" and presumptive identification of microcolonies was achieved here using existing publically available algorithms. Our system thus allows the growth of individual microcolonies to be monitored and critically, also to change the media during the growth phase without disrupting the microcolonies. Transfer of identified microcolonies onto selective media allowed us, within 1-2 bacterial generations, to rapidly detect the drug susceptibility of individual microcolonies, eliminating the need for time consuming subculturing or the inoculation of multiple parallel cultures. Significance: Monitoring the phenotype of individual microcolonies as they grow has immense potential for research, screening, and ultimately M. tuberculosis diagnostic applications. The method described is particularly appealing with respect to speed and automation

- 6 Tadrous, P.J. (2010)
Computer-Assisted Screening of Ziehl-Neelsen-Stained Tissue for Mycobacteria Algorithm Design and Preliminary Studies on 2,000 Images
American Journal of Clinical Pathology, 133, 849-858

Screening Ziehl-Neelsen (ZN)-stained sections for acid-alcohol-fast bacilli (AAFB) is laborious, and sparse bacilli are easily missed. This article presents an automatic screening algorithm using digital image analysis designed to assist human diagnosis of tissue sections. The algorithm uses multidervative source potentiators



and suppressors feeding into interconnected product nodes that result in a probability value for each image (the likelihood that it contains AAFB) and a spatial probability map showing the position of any bacillus. For the study, 3,000 images from ZN-stained tissues were captured, 1,000 were used to train the algorithm, and 2,000 were used to test it. The algorithm successfully ranked AAFB-containing images as the highest in the data sets, despite only single bacilli being present in sparse images (occupying 0.0024% of the image) and despite tissue and staining artifacts. These results suggest that this automated screening assistance method has the potential to save time and money, which is especially important in resource-poor health services

- 7 Williams, M.M., Yakrus, M.A., Arduino, M.J., Cooksey, R.C., Crane, C.B., Banerjee, S.N., Hilborn, E.D., Donlan, R.M. (2009)

Structural Analysis of Biofilm Formation by Rapidly and Slowly Growing Nontuberculous Mycobacteria

Applied and Environmental Microbiology, 75, 2091-2098

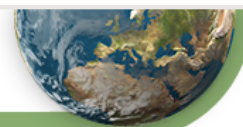
Mycobacterium avium complex (MAC) and rapidly growing mycobacteria (RGM) such as *M. abscessus*, *M. mucogenicum*, *M. chelonae*, and *M. fortuitum*, implicated in health care-associated infections, are often isolated from potable water supplies as part of the microbial flora. To understand factors that influence growth in their environmental source, clinical RGM and slowly growing MAC isolates were grown as biofilm in a laboratory batch system. High and low nutrient levels were compared, as well as stainless steel and polycarbonate surfaces. Biofilm growth was measured after 72 h of incubation by enumeration of bacteria from disrupted biofilms and by direct quantitative image analysis of biofilm microcolony structure. RGM biofilm development was influenced more by nutrient level than by substrate material, though both affected biofilm growth for most of the isolates tested. Microcolony structure revealed that RGM develop several different biofilm structures under high-nutrient growth conditions, including pillars of various shapes (*M. abscessus* and *M. fortuitum*) and extensive cording (*M. abscessus* and *M. chelonae*). Although it is a slowly growing species in the laboratory, a clinical isolate of *M. avium* developed more culturable biofilm in potable water in 72 h than any of the 10 RGM examined. This indicates that *M. avium* is better adapted for growth in potable water systems than in laboratory incubation conditions and suggests some advantage that MAC has over RGM in low-nutrient environments

- 8 Gulla, V., Banerjee, T., Patil, S. (2008)
Quantitative TLC analysis of steroid drug intermediates formed during bioconversion of soysterols
Chromatographia, 68, 663-667

A simple, rapid, and accurate method based on thin-layer chromatography (TLC) combined with image-analysis software has been developed for analysis of steroid drug intermediates formed during bioconversion of soysterols. The results obtained have been compared with those from LC. The method has been used to monitor the accumulation of widely used steroid drug intermediates androst-4-ene-3,17-dione (AD) and androsta-1,4-diene-3,17-dione (ADD), formed during the bioconversion of soysterols by *Mycobacterium* sp. NRRL B-3805 and *Mycobacterium* sp. NRRL B-3683. The percentage error between TLC and LC ranged between -0.79 to +4.50 for AD and -0.61 to +2.48 for ADD. Maximum conversion of soysterols to AD and ADD by *Mycobacterium* sp. NRRL B-3805 was 49.83 and 9.36 mol%, respectively, after incubation for 144 h, whereas conversion of soysterols by *Mycobacterium* sp. NRRL B-3683 after incubation 288 h was 41.90 mol% for AD and 37.79 mol% for ADD

- 9 Antunes, J.E., Freitas, M.P., da Cunha, E.F.F., Ramalho, T.C., Rittner, R. (2008)
In silico prediction of novel phosphodiesterase type-5 inhibitors derived from Sildenafil, Vardenafil and Tadalafil
Bioorganic & Medicinal Chemistry, 16, 7599-7606

A series of drug-like compounds derived from Sildenafil, Vardenafil and Tadalafil analogues were modelled through the MIA-QSAR (multivariate image analysis applied to quantitative structure-activity relationships) ligand-based approach. A highly predictive model was achieved and novel compounds, miscellany of substructures of these three representative phosphodiesterase type-5 (PDE-5) inhibitors were predicted using the calibration parameters obtained through partial least squares (PLS) regression. The high bioactivities of eight promising compounds were corroborated by docking evaluation. Calculated ADME-Tox (absorption, distribution, metabolism, excretion and toxicity) profiles for such compounds suggest advantages of some of them over the currently available, most common drugs used for the treatment of erectile dysfunction. (C) 2008 Elsevier Ltd. All rights reserved



- 10 Huang, T.S., Liu, Y.C., Bair, C.H., Sy, C.L., Chen, Y.S., Tu, H.Z., Chen, B.C. (2008)
Detection of M-tuberculosis using DNA chips combined with an image analysis system
International Journal of Tuberculosis and Lung Disease, 12, 33-38

OBJECTIVE: To develop a packaged DNA chip assay (the DR. MTBC Screen assay) for direct detection of the Mycobacterium tuberculosis complex. **DESIGN:** We described a DNA chip assay based on the IS6110 gene that can be used for the detection of M. tuberculosis complex. Probes were spotted onto the polystyrene strips in the wells of 96-well microtitre plates and used for hybridisation with biotin-labelled amplicon to yield a pattern of visualised positive spots. The plate image was scanned, analysed and interpreted automatically. **RESULTS:** The results corresponded well with those obtained by conventional culture as well as clinical diagnosis, with sensitivity and specificity rates of respectively 83.8% and 94.2%, and 84.6% and 96.3%. **CONCLUSION:** We conclude that the DR. MTBC Screen assay can detect M. tuberculosis complex rapidly in respiratory specimens, readily adapts to routine work and provides a flexible choice to meet different cost-effectiveness and automation needs in TB-endemic countries. The cost for reagents is around US\$10 per sample

- 11 Rocha, L.A., Vargas, P.A., Silva, L.F.F., Leon, J.E., Santos, A.B., Hiemstra, P.S., Mauad, T. (2008)
Expression of secretory leukocyte proteinase inhibitor in the submandibular glands of AIDS patients
Oral Diseases, 14, 82-88

OBJECTIVE: Secretory leukocyte proteinase inhibitor (SLPI) is an endogenous proteinase inhibitor present in mucosal secretions. It also displays antimicrobial activity including anti-human immunodeficiency virus activity. This protease inhibitor is also expressed in submandibular glands (SMG), but there are few data on its expression in AIDS patients with infectious conditions. **METHODS:** We analyzed the expression of SLPI using immunohistochemistry in submandibular gland samples of 36 AIDS patients [10 with normal histology, 10 with chronic nonspecific sialadenitis, eight with mycobacteriosis, and eight with cytomegalovirus (CMV) infection] and 10 HIV-negative controls. The proteinase inhibitor was quantified using image analysis and expressed as % of positively stained area. **RESULTS:** There was a higher expression of SLPI in AIDS patients with CMV infection (% of stained area, mean +/- SD: 37.37 +/- 14.45) when compared with all other groups (P = 0.009). There were no significant differences between control subjects (22.70 +/- 9.42%) and AIDS patients without histologic alterations (18.10 +/- 7.58%), with chronic nonspecific sialadenitis (17.13 +/- 5.36%), or mycobacterial infection (21.09 +/- 4.66%). **CONCLUSION:** Cytomegalovirus infection increases SLPI expression in the SMG of AIDS patients. Our results reveal new insights into the pathogenic association between HIV and CMV in AIDS patients

- 12 Yutkin, V., Pode, D., Pikarsky, E., Mandelboim, O. (2007)
The expression level of ligands for natural killer cell receptors predicts response to bacillus Calmette-Guerin therapy: A pilot study
Journal of Urology, 178, 2660-2664

Purpose: Up to 90% of patients with high grade superficial bladder tumors experience tumor recurrence and up to 50% have progression despite bacillus Calmette-Guerin treatment. Natural killer cells have a major role in the mechanism of the response to bacillus Calmette-Guerin but the exact mechanisms are still elusive. The recently discovered natural cytotoxicity receptors are linked to the host response to viral infection and to cancer. We tested the hypothesis that tumor expression of natural cytotoxicity receptor ligands can serve as a predictive factor for the response to intravesical bacillus Calmette-Guerin in patients with nonmuscle invasive, high grade bladder cancer. **Materials and Methods:** We developed a histochemical staining method for analysis of the ligands of the 3 known natural cytotoxicity receptors NKp30, NKp44 and NKp46 using genetically engineered fusion proteins and an automated image analysis system. We examined formalin fixed, paraffin embedded sections of specimens of transurethral bladder tumor resection from patients with primary, nonmuscle invasive, high grade bladder cancer who were subsequently treated with bacillus Calmette-Guerin. We compared natural cytotoxicity receptor ligand expression to the response to bacillus Calmette-Guerin immunotherapy. **Results:** Six of 17 patients (35%) had recurrence despite bacillus Calmette-Guerin treatment. Primary tumors from favorably responding patients expressed higher levels of ligands for all 3 fusion proteins (NKp30, NKp44 and NKp46 p = 0.0026, 0.027 and 0.044, respectively). **Conclusions:** Bacillus Calmette-Guerin resistant, high grade, nonmuscle invasive bladder tumors express significantly lower levels of ligands of all 3 natural cytotoxicity receptors compared with bacillus Calmette-Guerin responsive tumors. This suggests that down-regulation of these ligands facilitates escape from the bacillus Calmette-Guerin effect. Furthermore, analysis of ligand expression, which can be performed on formalin fixed, paraffin embedded sections, may serve as a new predictive assay for the response to bacillus Calmette-Guerin



- 13 Fumuso, E.A., Aguilar, J., Giguere, S., Rivulgo, M., Wade, J., Rogan, D. (2007)
Immune parameters in mares resistant and susceptible to persistent post-breeding endometritis: Effects of immunomodulation
Veterinary Immunology and Immunopathology, 118, 30-39

Our objective was to characterize immune parameters in susceptible (SM) and resistant (RM) mares, with and without artificial insemination (AI) and immunomodulation. Eight RM and eight SM were selected based on their reproductive history and functional tests. Both groups of mares were evaluated during three consecutive cycles: Cycle 1, untreated cycle (control); Cycle 2, AI with dead semen; Cycle 3, AI with dead semen and immunomodulation. Endometrial biopsies were taken during the three cycles as follows: Cycle 1 - at estrus, when follicles ≥ 35 mm and at diestrus (7 \pm 1 days after ovulation); Cycle 2-at estrus 24 h post-AI, and at diestrus; Cycle 3-at estrus 24 h after treatment with a *Mycobacterium phlei* cell-wall extract (MCWE) and AI, and at diestrus. The mRNA transcription (mRNAT) of IL-8 and IL-10 were determined by real-time PCR. Image analysis of immunohistochemistry slides was performed using digital software (Image-Pro Plus v 5.0; Media Cybernetics); the percentage of stained area was determined for Major Histocompatibility Complex II (MHC-II), polymorphonuclear leukocytes (PMN) and T lymphocytes (TL) on each tissue section. In Cycle 1, SM had significantly higher MHC-II, TL, PMN and IL-8 than RM during estrus ($P < 0.006$, $P < 0.0005$, $P < 0.05$, respectively), while transcription of IL-10 was significantly lower than in RM ($P < 0.0001$). During diestrus, SM had higher levels of TL, PMN and IL-8 than RM ($P < 0.0001$). After AI (Cycle 2), SM had higher levels of IL-8 and lower levels of IL-10 than RM at estrus and no differences were detected for MHC-II, TL and PMN positive cells. During diestrus in the same cycle, all the immune parameters were higher in SM mares ($P < 0.005$, $P < 0.0004$, $P < 0.0001$, $P < 0.02$, respectively). When MCWE was applied at the time of AI (Cycle 3), SM expressed significant higher levels of IL-10 24 h after treatment ($P < 0.005$), which were also higher than in the control Cycle 2 or after AI (Cycle 2). However, no significant differences were detected for MHC-II, lymphocytes-PMN or IL-8 between SM and RM during diestrus in Cycle 3. This study showed that SM had higher levels of all immune parameters except IL-10 than RM during Cycle 1. After AI (Cycle 2), the inflammatory condition persisted in SM but not RM mares until day 7 post-ovulation. Following treatment with MCWE at the time of AI (Cycle 3) uterine immunological changes in SM resulted in an endometrial immune environment similar to that found in normal RM. (c) 2007 Elsevier B.V. All rights reserved

- 14 Lousada, S., Florido, M., Appelberg, R. (2006)
Regulation of granuloma fibrosis by nitric oxide during *Mycobacterium avium* experimental infection
International Journal of Experimental Pathology, 87, 307-315

Collagen deposition within granulomas formed after *Mycobacterium avium* infection was analysed on histological sections stained with Masson's trichrome using acquired computerized image analysis and a program that was specifically designed for that purpose. Comparison was made between immunocompetent C57BL/6 mice and mice genetically deficient in the inducible nitric oxide (NO) synthase gene (iNOS(-/-) mice) infected with either a highly virulent strain or a moderately virulent strain of *M. avium*. iNOS-deficient mice were more resistant to the highly virulent strain than control C57BL/6 mice, but both strains were equally susceptible to the less virulent *M. avium* strain. Collagen distribution in the granuloma was found in the cuff surrounding the granuloma in an area rich in lymphoid cells as well as inside the granuloma itself, conferring a mesh-like structure within that lesion. It was seen that iNOS(-/-) mice induced a higher collagen deposition than C57BL/6 mice and that such collagen deposition varied with the mycobacterial strain used to infect the animals

- 15 Forero, M.G., Cristobal, G., Desco, M. (2006)
Automatic identification of *Mycobacterium tuberculosis* by Gaussian mixture models
Journal of Microscopy-Oxford, 223, 120-132

Tuberculosis and other kinds of mycobacteriosis are serious illnesses for which early diagnosis is critical for disease control. Sputum sample analysis is a common manual technique employed for bacillus detection but current sample-analysis techniques are time-consuming, very tedious, subject to poor specificity and require highly trained personnel. Image-processing and pattern-recognition techniques are appropriate tools for improving the manual screening of samples. Here we present a new technique for sputum image analysis that combines invariant shape features and chromatic channel thresholding. Some feature descriptors were extracted from an edited bacillus data set to characterize their shape. They were statistically represented by using a Gaussian mixture model representation and a minimal error Bayesian classification procedure was employed for the last identification stage. This technique constitutes a step towards automating the process and providing a high specificity



- 16 Schmidt, F., Dahlmann, B., Janek, K., Kloss, A., Wacker, M., Ackermann, R., Thiede, B., Jungblut, P.R. (2006)
Comprehensive quantitative proteome analysis of 20S proteasome subtypes from rat liver by isotope coded affinity tag and 2-D gel-based approaches
Proteomics, 6, 4622-4632

Quantitative protein profiling is an essential part of proteomics and requires technologies that accurately, reproducibly, and comprehensively identify and quantify proteins. Over the past years, many quantitative proteomic methods have been developed. Here, 20S proteasome subtypes isolated from rat were compared by four approaches based on the combination of isotope-coded affinity tag (ICAT), 2-DE, LC and ESI and MALDI MS: (i) 2-DE, (ii) ICAT/2-DE MALDI-MS, (iii) ICAT/LC-ESI-MS, (iv) ICAT/LC-MALDI-MS. A definite qualitative advantage of 2-DE gels was the separation of all known protein species, the identification of cysteine sulfoxide of alpha-4 (RC6-IS) and N-terminal acetylation of several subunits. Furthermore, quantitative differences between the standard subunits beta-2, and beta-5 and their immunosubunits were only detected by 2-DE image analysis revealing a higher replacement of standard- by immuno-beta-subunits in subtype IV. It was obvious that for relative quantification only protein spot and mass peaks with a certain level of intensity displayed acceptable values of SD. However, ICAT in conjunction with LC/MALDI-MS was the most accurate method for quantification.

- 17 Mattow, J., Demuth, I., Haeselbarth, G., Jungblut, P.R., Klose, J. (2006)
Selenium-binding protein 2, the major hepatic target for acetaminophen, shows sex differences in protein abundance
Electrophoresis, 27, 1683-1691

Liver samples from female and male mice of two subspecies, *Mus musculus musculus* and *Mus musculus domesticus*, were investigated by a combination of 2-DE and MALDI-MS. The image analysis of the generated 2-DE patterns revealed several protein spots with significant differences in intensity/abundance between the sexes. Seven protein spots, which were prominent in 2-DE patterns of male mice, but which showed very low intensities in females, were identified as selenium-binding protein 2 (SBP2) also known as 56-kDa acetaminophen-binding protein. Edman degradation indicated that at least three of these protein spots represent N-terminally truncated SBP2 variants. Furthermore, it was shown that the observed differences in SBP2 abundance correlate with sex differences in transcription of the gene encoding SBP2, *selenbp2*, as revealed by RT-PCR and restriction digest as well as sequence analysis of the products. Since SBP2 has been described as the major target for acetaminophen in mouse liver cytosol, these findings are discussed with respect to their possible relevance for sex differences in acetaminophen-mediated toxicity, which have been described in a variety of mammals including mice and rats.

- 18 Stephan, J., Bender, J., Wolschendorf, F., Hoffmann, C., Roth, E., Mailander, C., Engelhardt, H., Niederweis, M. (2005)
The growth rate of *Mycobacterium smegmatis* depends on sufficient porin-mediated influx of nutrients
Molecular Microbiology, 58, 714-730

Mycobacteria have a unique outer membrane (OM) that is thicker than any other known biological membrane. Nutrients cross this permeability barrier by diffusion through porins. MspA is the major porin of *Mycobacterium smegmatis*. In this study we showed that three paralogues of MspA, namely MspB, MspC and MspD are also porins. However, only the *mspA* and *mspC* genes were expressed in the wild-type strain. None of the single deletion mutants displayed a significant OM permeability defect except for the *mspA* mutant. Deletion of the *mspA* gene caused activation of transcription of *mspB* and/or *mspD* in three independent strains by unknown chromosomal mutations. It is concluded that *mspB* and *mspD* provide backup porins for *M. smegmatis*. This also indicated that a minimal porin-mediated OM permeability is essential for survival of *M. smegmatis*. Electron microscopy in combination with quantitative image analysis of protein gels revealed that the number of pores per cell dropped from 2400 to 800 and 150 for the Delta *mspA* and Delta *mspA* Delta *mspC* mutant (ML10) respectively. The very low number of pores correlated well with the at least 20-fold lower channel activity of detergent extracts of the ML10 strain and its 15- and 75-fold lower permeability to nutrient molecules such as serine and glucose respectively. The amount of Msp porin and the OM permeability of the triple porin mutant lacking *mspA*, *mspC* and *mspD* was not altered. The growth rate of *M. smegmatis* dropped drastically with its porin-mediated OM permeability in contrast to porin mutants of *Escherichia coli*. These results show that porin-mediated influx of nutrients is a major determinant of the growth rate of *M. smegmatis*.



- 19 Torocsik, D., Bardos, H., Nagy, L., Adany, R. (2005)
Identification of factor XIII-A as a marker of alternative macrophage activation
Cellular and Molecular Life Sciences, 62, 2132-2139

Factor XIII subunit A of blood coagulation (FXIII-A) is known to be synthesized but not secreted by the monocyte/macrophage cell line. On the basis of its intracellular localization and substrate profile, FXIII-A is thought to be involved in certain intracellular processes. Our present study was designed to monitor the changes in FXIII-A gene expression and protein production in long-term culture of human monocytes during their differentiation into macrophages in the presence of activating agents (interleukin-4, interferon-gamma, Mycobacterium bovis BCG) inducing classical and alternative activation pathways. By using quantitative RT-PCR and fluorescent image analysis at the single-cell level we demonstrated that the expression of FXIII-A both at the mRNA as well as at the protein level is inversely regulated during the two activation programmes. Here we conclude that FXIII-A expression is an intracellular marker for alternatively activated macrophages, while its absence in monocyte-derived macrophages indicates their classically activated state

- 20 De Rycke, L., Vandooren, B., Kruihof, E., De Keyser, F., Veys, E.M., Baeten, D. (2005)
Tumor necrosis factor a blockade treatment down-modulates the increased systemic and local expression of toll-like receptor 2 and toll-like receptor 4 in spondylarthropathy
Arthritis and Rheumatism, 52, 2146-2158

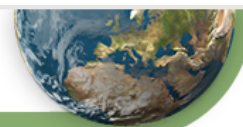
Objective. Abnormal host defense against pathogens has been implicated in the pathogenesis of spondylarthropathy (SpA), a disease characterized by abundant synovial infiltration with innate immune cells. Given the role of Toll-like receptors (TLRs) in activation of innate inflammation and the occurrence of TLR-dependent infections after tumor necrosis factor alpha (TNF alpha) blockade treatment, the present study was undertaken to analyze TLRs and their modulation by TNF alpha blockade in SpA. Methods. Peripheral blood mononuclear cells (PBMCs) were obtained from SpA and rheumatoid arthritis (RA) patients during infliximab therapy, and from healthy controls. TLR-2 and TLR-4 expression and TNF α production upon lipopolysaccharide (LPS) stimulation were analyzed by flow cytometry on different monocyte subsets. Synovial biopsy specimens from 23 SpA patients before and after infliximab or etanercept treatment, from 15 RA patients, and from 18 osteoarthritis (OA) patients were analyzed by immunohistochemistry. Results. Expression of TLR-4, but not TLR-2, was increased on PBMCs from patients with SpA, whereas both TLRs were increased in RA patients. TLR expression was particularly increased on the CD163+ macrophage subset. Infliximab reduced TLR-2 and TLR-4 expression on monocytes of SpA and RA patients, leading to lower levels than in controls and to impaired TNF α production upon LPS stimulation. In inflamed synovium, the expression of both TLRs and of CD163 was significantly higher in patients with SpA than in those with RA or OA. Paralleling the systemic effect, TLRs in synovium were down-regulated following treatment with infliximab as well as etanercept, indicating a class effect of TNF α blockers. Conclusion. Inflammation in SpA is characterized by increased TLR-2 and TLR-4 expression, which is sharply reduced by TNF α blockade. These findings suggest a potential role of innate immunity-mediated inflammation in SpA and provide an additional clue regarding the mechanism of action as well as the potential side effects of TNF α blockade

- 21 Lamonica, J.M., Wagner, M.A., Eschenbrenner, M., Williams, L.E., Miller, T.L., Patra, G., DeVecchio, V.G. (2005)
Comparative secretome analyses of three Bacillus anthracis strains with variant plasmid contents
Infection and Immunity, 73, 3646-3658

Bacillus anthracis, the causative agent of anthrax, secretes numerous proteins into the extracellular environment during infection. A comparative proteomic approach was employed to elucidate the differences among the extracellular proteomes (secretomes) of three isogenic strains of B. anthracis that differed solely in their plasmid contents. The strains utilized were the wild-type virulent B. anthracis RA3 (pXO1(+) pXO2(+)) and its two nonpathogenic derivative strains: the toxigenic, nonencapsulated RA3R (pXO1(+) pXO2(-)) and the totally cured, nontoxigenic, nonencapsulated RA3:00 (pXO1(-) pXO2(-)). Comparative proteomics using two-dimensional gel electrophoresis followed by computer-assisted gel image analysis was performed to reveal unique, up-regulated, or down-regulated secretome proteins among the strains. In total, 57 protein spots, representing 26 different proteins encoded on the chromosome or pXO1, were identified by peptide mass fingerprinting. S-layer-derived proteins, such as Sap and EA1, were most frequently observed. Many sporulation-associated enzymes were found to be overexpressed in strains containing pXO1(+). This study also provides evidence that pXO2 is necessary for the maximal expression of the pXO1-encoded toxins lethal factor (LF), edema factor (EF), and protective antigen (PA). Several newly identified putative virulence factors were observed; these include enolase, a high-affinity zinc uptake transporter, the peroxide stress-related alkyl hydroperoxide reductase, isocitrate lyase, and the cell surface protein A



- 22 Pleissner, K.P., Schmelzer, P., Wehr, W., Jungblut, P.R. (2004)
Presentation of differentially regulated proteins within a web-accessible proteome database system of microorganisms
Proteomics, 4, 2987-2990
- Web-accessible proteome databases represent indispensable tools for quantitative and comparative proteomics research. The majority of two-dimensional gel electrophoresis (2-DE) databases contains clickable 2-DE gel images and descriptive textual information such as protein name, M-r/p/l values, methods of identification, cellular localization and other information on proteins. Although a great part of the work in comparative proteomics consists of the analysis of 2-DE gels using image analysis approaches, most proteome databases lack the ability to present protein abundance data and their alterations within experiments via the web. Now, differentially regulated proteins detected in microbial experiments by quantitative gel image analysis are presented in a web-accessible relational database DIFF (Differentially Regulated Proteins). The DIFF database is a part of the proteome database system for microbial research available at <http://www.mpiib-berlin.mpg.de/2D-PAGE>
- 23 Forero, M.G., Sroubek, F., Cristobal, G. (2004)
Identification of tuberculosis bacteria based on shape and color
Real-Time Imaging, 10, 251-262
- Tuberculosis and other mycobacteriosis are serious illnesses which control is based on early diagnosis. A technique commonly used consists of analyzing sputum images for detecting bacilli. However, the analysis of sputum is time consuming and requires highly trained personnel to avoid high errors. Image-processing techniques provide a good tool for improving the manual screening of samples. In this paper, a new autofocus algorithm and a new bacilli detection technique is presented with the aim to attain a high specificity rate and reduce the time consumed to analyze such sputum samples. This technique is based on the combined use of some invariant shape features together with a simple thresholding operation on the chromatic channels. Some feature descriptors have been extracted from bacilli shape using an edited dataset of samples. A k-means clustering technique was applied for classification purposes and the sensitivity vs specificity results were evaluated using a standard ROC analysis procedure. (C) 2004 Elsevier Ltd. All rights reserved
- 24 De Carvalho, C.C.C.R., Da Cruz, A.A.R.L., Pons, M.N., Pinheiro, H.M.R.V., Cabral, J.M.S., Da Fonseca, M.M.R., Ferreira, B.S., Fernandes, P. (2004)
Mycobacterium sp., Rhodococcus erythropolis, and Pseudomonas putida behavior in the presence of organic solvents
Microscopy Research and Technique, 64, 215-222
- This work aimed at studying the behavior and tolerance of Mycobacterium sp. NRRL B-3805, Rhodococcus erythropolis DCL14 and Pseudomonas putida S 12 cells in the presence of various concentrations of water miscible (ethanol, butanol, and dimethylformamide, up to 50% v/v) and water immiscible solvents (dodecane, bis(2-ethylhexyl) phthalate and toluene, up to 5% v/v). When incubated in the presence of these solvents, the cells were found to have lower tolerance to butanol and toluene than to the remaining solvents. Nevertheless, the concentrations of solvents endured by the tested strains show that they are quite solvent-tolerant, confirming their potential as biocatalysts in nonconventional systems. Microscopic observation of samples showed that the hydrophobic Mycobacterium sp. and R. erythropolis cells were able to aggregate to protect the population under stress conditions. Comparison of the results obtained at the single cell level by fluorescence microscopy and colony development on agar plates indicated that the primary effects of most solvents tested were on the cell membrane and replicating capability of the cells. (C) 2004 Wiley-Liss, Inc
- 25 De Carvalho, C.C.C.R., Da Fonseca, M.M.R. (2004)
Principal component analysis applied to bacterial cell behaviour in the presence of organic solvents
Biocatalysis and Biotransformation, 22, 203-214
- The behaviour of cells of Rhodococcus erythropolis DCL14, Xanthobacter Py2, Arthrobacter simplex and Mycobacterium sp. NRRL B-3805, in biphasic systems containing different organic solvents was evaluated and compared. The data, obtained mainly by fluorescence microscopy and image analysis, was interpreted using principal components analysis (PCA). With this technique, the variability of the data could be summarised in 7 components, representing 75.8% of the variance of the data. Over a third of the variance could be explained by the first two principal components which represent solvent toxicity. Apparently this is the major factor influencing cell behaviour in an organic:aqueous system. However, factors such as substrate concentration, cell adaptation ability (resulting in morphological changes and aggregation or separation of cells) and membrane composition (specific to each strain) also play an important role in cell resistance to solvent toxicity. The results regarding cell shape indicate that loss of viability occurs, in the tested bacterial



strains, after incorporation of molecules of solvent in the cellular membrane. This should result in an increase in membrane fluidity, and thus, in an alteration of cell shape. The ability to form "self-defence" clusters was observed to be different amongst the four strains. X. Py2 showed, in general, a low tendency to form aggregates under the tested conditions; A. simplex and R. erythropolis aggregated mainly in the presence of low log P solvents; and Mycobacterium sp. cells showed a high ability to aggregate

- 26 Harms, C.A., Howard, K.E., Wolf, J.C., Smith, S.A., Kennedy-Stoskopf, S. (2003)
Transforming growth factor-beta response to mycobacterial infection in striped bass *Morone saxatilis* and hybrid tilapia *Oreochromis spp*
Veterinary Immunology and Immunopathology, 95, 155-163

Striped bass (*Morone saxatilis*) and hybrid tilapia (*Oreochromis spp.*) were experimentally infected with *Mycobacterium marinum*. Splenic mononuclear cell transforming growth factor-beta (TGF-beta) mRNA was measured by reverse transcription quantitative-competitive PCR (RT-qcPCR). In histologic sections of liver and anterior kidney, the area of each section that was occupied by granulomas and the total area of each section were measured by computer-assisted image analysis and compared as a proportion (the granuloma proportion). Infected striped bass splenic, mononuclear cell TGF-beta mRNA expression was significantly lower than uninfected controls, while for tilapia there was no significant difference between infected and control fish. Mycobacterial granuloma proportion of liver and anterior kidney sections was significantly greater for infected striped bass than tilapia. Three (of 10) infected tilapia with the most pronounced inflammatory response displayed a decrease in TGF-beta mRNA expression, similar to the overall striped bass response to mycobacterium challenge. Downregulation of TGF-beta and failure to modulate the immune response may be related to excessive inflammatory damage to organs observed in mycobacteria-sensitive fish species. (C) 2003 Elsevier B.V. All rights reserved

- 27 Maithal, K. (2002)
Proteomics - A new player in the post-genomic era
Indian Journal of Biochemistry & Biophysics, 39, 291-302

In the post-genomic era the concept of personalized medicine and molecular medicine emphasizes the utility of the proteomics approach. Proteomics is the global analysis of cellular proteins and complements the genomics approach. Proteins, in principle do all the work of the cell and ultimately dictate all biological processes and the cellular fate. Proteomics uses a combination of sophisticated techniques including two-dimensional (2D) gel electrophoresis, image analysis, mass spectrometry, amino acid sequencing and bioinformatics to identify and characterize proteins. This review aims at providing the various approaches and pitfalls associated with this technique and gives a brief overview of the utility of this approach in the area of biomedical research

- 28 Hrabec, E., Strek, M., Zieba, M., Kwiatkowska, S., Hrabec, Z. (2002)
Circulation level of matrix metalloproteinase-9 is correlated with disease severity in tuberculosis patients
International Journal of Tuberculosis and Lung Disease, 6, 713-719

SETTING: Parenchymal lung destruction accompanied by active tuberculosis is, at least in part, caused by host as well as bacillus metalloproteinases. *Mycobacterium tuberculosis* has been shown to stimulate MMP-9 expression in the lung of infected organisms. DESIGN: We have used quantitative zymography and computer-assisted image analysis to measure the levels of type IV collagenases in 20 serum samples of patients with active tuberculosis and in 23 serum samples of healthy volunteers. RESULTS: Mean levels of the serum MMP-9 were over three-fold higher in tuberculous samples compared with normal serum ($P < 0.0001$), whereas the MMP-2 levels did not differ in these two groups. The levels of MMP-9 were significantly higher in subjects with advanced disease than in those with only limited disease changes ($P < 0.05$). CONCLUSIONS: We suppose that the elevation of serum MMP-9 levels in patients with tuberculosis is affected by the augmentation of synthesis and/or secretion of this enzyme by inflammatory cells in response to *M. tuberculosis* infection. The observed association between the serum MMP-9 level and the extent of radiological change suggests that the quantification of the serum level of this enzyme may constitute a supplementary test-in pulmonary tuberculosis diagnostics

- 29 Palmer, M.V., Gosch, G., Lyon, R., Waters, W.R., Whipple, D.L. (2002)
Apoptosis in lymph node granulomas from white-tailed deer (*Odocoileus virginianus*) experimentally infected with *Mycobacterium bovis*
Journal of Comparative Pathology, 127, 7-13

Apoptosis is a morphologically and biochemically distinct mechanism of cell death seen in many physiological conditions as well as in various infectious diseases. To examine apoptosis in tuberculous white-tailed deer,



32 deer were each given an intra-tonsillar injection of 300 colony-forming units of *Mycobacterium bovis*. Medial retropharyngeal lymph nodes were collected at 15, 28, 42, 56, 89, 180, 262 and 328 days after inoculation. Microscopical sections of lymph nodes were labelled for apoptotic cells by the terminal deoxynucleotidyl transferase nick end labelling (TUNEL) method. TUNEL, and other morphological changes within developing granulomas, were analysed and quantified by computerized image analysis. TUNEL within granulomas was greatest 28 days after inoculation and had declined to negligible levels by 328 days. Granuloma enlargement was due primarily to an increase in size of the caseo-necrotic core of the granuloma and not to increased inflammatory cellular infiltrate. These findings suggested that cell death within *M. bovis*-induced granulomas in white-tailed deer was due mainly to mechanisms other than apoptosis. (C) 2002 Published by Elsevier Science Ltd

- 30 Meas-Yedid, V., Tilie, S., Olivo-Marin, J.C. (2002)
Color image segmentation based on Markov Random Field Clustering for histological image analysis
16Th International Conference on Pattern Recognition, Vol I, Proceedings, 796-799

In order to characterise the virulence factors of different *Mycobacterium tuberculosis* strains responsible of tuberculosis disease, the quantification, by cell counting, of immune cell recruitment is necessary. However this task by microscopic observations is very tedious and difficult to reproduce. Hence we propose an automatic counting approach, consisting in color image segmentation to discriminate three regions: cell nuclei, immune cells and background, followed by the extraction of each cell entity,. For color segmentation, a Markov Random Field Clustering approach taking simultaneously into account both color and spatial information is chosen. Our technique was successfully applied to several color images of different strains, and an evaluation of the results has been performed, showing the robustness of the method against noise, marker color changes, illumination changes and blurring

- 31 Paolicchi, F.A., Vagnozzi, A., Morsella, C.G., Verna, A.E., Massone, A.R., Portiansky, E.L., Gimeno, E.J. (2001)
Paratuberculosis in red deer (*Cervus elaphus*): an immunohistochemical study
Journal of Veterinary Medicine Series B-Infectious Diseases and Veterinary Public Health, 48, 313-320

In the present study, we compared the utility of immunohistochemistry with serological and histological results for the characterization of *Mycobacterium avium* ssp. paratuberculosis (*M. paratuberculosis*) in tissues of affected red deer. Bacterial isolation was considered the standard reference. Samples were taken from seven clinically affected animals with typical macroscopic lesions. The enzyme linked immunosorbent assay (ELISA) and the gel diffusion tests (GD) were used for serological determinations. Samples from intestine and mesenteric lymph nodes were processed for bacterial isolation and histology. *M. paratuberculosis* was isolated from all the animals. Histologically, lymph nodes displayed necrosis and mineralization at the cortical and medullar areas. Ziehl-Neelsen stained bacteria were numerous inside macrophages and Langhans-type giant cells. Giant and epithelioid cells and lymphocytes were prominent at the ileal mucous membrane. The immunostaining of *M. paratuberculosis* was very clear inside epithelioid and giant cells. Image analysis was carried out to determine the immunostained area. There was total agreement among the methods employed. Immunohistochemistry can be very useful when the microorganism cannot be recovered from tissues or faeces

- 32 Borrego, S., Niubo, E., Ancheta, O., Espinosa, M.E. (2000)
Study of the microbial aggregation in mycobacterium using image analysis and electron microscopy
Tissue & Cell, 32, 494-500

Cellular aggregation, which occurs in both prokaryotes and eukaryotes, is controlled by the hydrophobicity as well as the electrokinetic potential of the cell surface and substratum. It is known that the *Mycobacterium* genus form aggregates, but the influence of sugar on the cellular aggregation has not been reported for this genus. The mutant strain *Mycobacterium* sp, MB-3683 that transforms sterol to androstendione (AD), a steroidal precursor used by the pharmaceutical industries, was employed in this study. This strain was cultivated in a synthetic medium on three sugars (glycerol, glucose and fructose) at different concentrations, and at 144 h microbial growth, cellular aggregation, hydrophobicity, lipid content, fatty acid composition, and width of cellular walls were measured. It was observed that at different sugar concentrations, similar growth and pH were obtained. However, in fructose, the aggregation level was significantly high, followed by glycerol and glucose (fructose < glycerol < glucose). These results were confirmed using electron microscopy and the aggregate area quantified by image analysis. Hydrophobicity was the highest in fructose and the lowest in glucose. The total lipids, in contrast to cellular hydrophobicity, were higher in glucose than glycerol. Although, the hydrophilic-lipophilic balance (HLB) of principal fatty acids isolated was similar regardless of sugar used. In glycerol and fructose, the paraffins were observed, which are responsible for the high cellular hydrophobicity detected above. The width of cell wall of the organisms grown on glucose and fructose was



similar, but in glycerol the walls were very thin. There is a correspondence between cell wall width and lipid content. (C) 2000 Harcourt Publishers Ltd

- 33 Barrett, J., Jefferies, J.R., Brophy, P.M. (2000)
Parasite proteomics
Parasitology Today, 16, 400-403

Proteomics offers a new set of tools for investigating parasites and parasite-associated disease. In this article, John Barrett, Jim Jefferies and Peter Brophy describe the key technologies involved, including two-dimensional gel electrophoresis, image analysis, biological mass spectroscopy and database searching. The potential applications of proteomics in drug and vaccine discovery are reviewed, as are possible future developments

- 34 Walker, J.T., Bradshaw, D.J., Bennett, A.M., Fulford, M.R., Martin, M.V., Marsh, P.D. (2000)
Microbial biofilm formation and contamination of dental-unit water systems in general dental practice
Applied and Environmental Microbiology, 66, 3363-3367

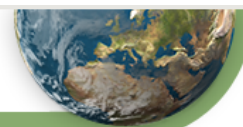
Dental-unit water systems (DUWS) harbor bacterial biofilms, which may serve as a haven for pathogens. The aim of this study was to investigate the microbial load of water from DUWS in general dental practices and the biofouling of DUWS tubing. Water and tube samples were taken from 55 dental surgeries in southwestern England. Contamination was determined by viable counts on environment ally selective, clinically selective, and pathogen-selective media, and biofouling was determined by using microscopic and image analysis techniques. Microbial loading ranged from 500 to 10(5) CFU . ml(-1); in 95% of DUWS water samples, it exceeded European Union drinking water guidelines and in 83% it exceeded American Dental Association DUWS standards. Among visible bacteria, 68% were viable by BacLight staining, but only 5% of this "viable by BacLight" fraction produced colonies on agar plates. Legionella pneumophila, Mycobacterium spp., Candida spp., and Pseudomonas spp, were detected in one, five, two, and nine different surgeries, respectively. Presumptive oral streptococci and Fusobacterium spp, mere detected in four and one surgeries, respectively, suggesting back siphonage and failure of antiretraction de,ices. Hepatitis B virus was never detected. Decontamination strategies (5 of 55 surgeries) significantly reduced biofilm coverage but not significantly increased microbial numbers in the water phase (in both cases, P < 0.05), Microbial loads were not significantly different in DUWS fed with soft, hard, deionized, or distilled water or in different DUWS (main, tank, or bottle fed). Microbiologically, no DUWS can be considered "cleaner" than others. DUWS deliver water to patients with microbial levels exceeding those considered safe for drinking water

- 35 Carol, M., Pelegri, C., Castellote, C., Franch, A., Castell, M. (2000)
Immunohistochemical study of lymphoid tissues in adjuvant arthritis (AA) by image analysis; relationship with synovial lesions
Clinical and Experimental Immunology, 120, 200-208

The aim of this study was to examine leucocyte populations in lymphoid organs during AA and to ascertain the relationship with lesions in synovial joints. Popliteal lymph nodes, spleen and knee synovial membranes were removed from both healthy and AA rats at intervals of 3-4 days over a 3-week period. Cryostat sections were stained with MoAbs directed against lymphocyte and macrophage subpopulations, and studied by image analysis. Throughout the arthritic period, high numbers of ED1(+) and ED3(+) macrophages were seen in both lymphoid compartments and intercellular adhesion molecule-1 (ICAM-1) expression also increased in some zones of lymph nodes and spleen. The percentages of CD4(+) and CD8(+) cells rose in the splenic zones studied but fell in the lymph node cortex. Very few natural killer (NK) cells were found in lymphoid tissues, but the number rose after AA induction. In synovia from AA rats, ED2(+) macrophages proliferated but alpha/beta T cell infiltration was only occasionally observed, accompanied by ED1(+) cells and ICAM-1 expression. In conclusion, synovitis developing after AA induction seems to be caused directly by macrophages and indirectly by lymphocytes placed both in popliteal lymph nodes and spleen

- 36 Li, Q.S., Mansfield, K.G., Lackner, A.A., Haase, A.T. (2000)
Quantitative image analysis of simian immunodeficiency virus replication in macrophages coinfectd with Mycobacterium avium complex
Journal of Infectious Diseases, 181, 867-871

Mycobacterium avium is the most frequent cause of disseminated bacterial infection in patients with human immunodeficiency virus type 1 infection and in rhesus macaques with simian immunodeficiency virus (SIV) infection. This animal model of AIDS was used to test the hypothesis that this frequent association is the result of reciprocal enhancement of replication of both microorganisms, The replication of M. avium and SN was analyzed in lymphatic tissues obtained from rhesus macaques experimentally inoculated with SIVmac who developed or remained free of overt M. avium infection. In situ hybridization, quantitative image analysis,



and staining of *M. avium* and of macrophages were used to assess the effects of coinfection on the replication of SIV and *M. avium* in vivo. There was no correlation between virus load and *M. avium* load in coinfecting lymph nodes, and, with one exception, there was no evidence that *M. avium* coinfection of macrophages increased SIV replication

- 37 Matsunaga, K., Ito, M. (2000)
Quantitative analysis of apoptotic cell death in granulomatous inflammation induced by intravenous challenge with *Cryptococcus neoformans* and bacillus Calmette-Guerin vaccine
Pathology International, 50, 206-218

Apoptotic cell death of macrophage has become recognized as a significant mechanism responsible for the resolution of inflammation. The purpose of this study was to examine how the apoptotic cell death involves the formation and resolution of granulomas in rats intravenously inoculated with *Cryptococcus neoformans* (*Cr. neoformans*) and *Mycobacterium bovis*-derived bacillus Calmette-Guerin (BCG) vaccine. The number and size of granulomas in the livers obtained on days 5, 10, 15, 20 and 25 after inoculation were examined by morphometric image analysis, as well as the occurrence of apoptotic cell death quantitatively analyzed by terminal deoxynucleotidyl transferase (TdT)-mediated dUTP-biotin nick end-labeling (TUNEL) procedure on tissue sections. In both groups the number and size of granulomas were maximized on day 10, then the granulomas were almost resolved until day 25 when the inoculated *Cr. neoformans* and BCG almost disappeared. From the induction to the resolving stages of granulomatous inflammation, TUNEL-positive cells constantly appeared in granulomas, and the highest frequency of apoptotic cells in granulomas was observed in the earlier stage of granuloma formation. These results indicate that the maintenance and resolution of infectious granulomas are regulated by the balance between the influx of newly recruited macrophages and the apoptotic elimination of granuloma macrophages. The apoptosis of granuloma macrophages actively involves the cellular turnover in both granuloma formation and resolution

- 38 Bhat, M., Hickey, A.J. (2000)
Effect of chloroquine on phagolysosomal fusion in cultured guinea pig alveolar macrophages: Implications in drug delivery

Aaps Pharmsci, 2, The aim of this study was to evaluate the effects of chloroquine on phagolysosomal fusion (PLF) in cultured guinea pig alveolar macrophages (AMs). This technique may be of significance for antitubercular drugs, because the survival of *Mycobacterium tuberculosis* is linked to evasion of PLF. Guinea pig AMs were obtained from anesthetized animals after exsanguination. The AMs were cultured at a density of 1×10^6 cell/mL in 24-well plates after attachment to 13-mm coverslips. Culture conditions were at 37 degreesC, with 95% air/5% C-O₂ in Roswell Park Memorial Institute (RPMI) 1640 medium with 10% heat-inactivated fetal bovine serum. Rhodamine-dextran (70 kd) was incubated with the cells at 0.25 mg/mL for 24 hours to label the lysosomes. Chloroquine treatment where indicated was performed at 10-20 μ g/mL for 1 hour. Fluorescent BioParticles were then added, and PLF was monitored by formation of an orange-yellow fluorescence on fusion of green fluorescent BioParticles with rhodamine-labeled lysosomes. PLF endpoints were measured by scoring for the percentage of orange-yellow cells in the field of view. Image analysis to measure the intensity of the orange-yellow color was performed by obtaining a, b values for 5 x 5 pixel areas using the PhotoAdobe program 4.0.1. The results indicated that the rate of PLF was enhanced by chloroquine. Thus, chloroquine may be used to potentiate the effects of rifampicin. This may be confirmed by studies involving similar dual fluorophore labeling techniques of fluorescein-labeled formulation in macrophages infected with *M. tuberculosis*. Preliminary studies with the rhodamine-labeled formulation confirmed cellular uptake and persistence for up to 7 days in culture

- 39 Knoell, T., Safarik, J., Cormack, T., Riley, R., Lin, S.W., Ridgway, H. (1999)
Biofouling potentials of microporous polysulfone membranes containing a sulfonated polyether-ethersulfone/polyethersulfone block copolymer: correlation of membrane surface properties with bacterial attachment
Journal of Membrane Science, 157, 117-138

Multivariate methods were used to identify relationships between bacterial attachment (biofouling potential), water transport, and the surface properties of nine modified polysulfone (MPS) membranes comprising blends of polysulfone (PS) with a sulfonated polyether-ethersulfone/polyethersulfone block copolymer. The topology of the microporous MPS membranes, including surface roughness, surface height, pore size and pore geometry were determined by atomic force microscopy (AFM) and digital image analysis. Other measurements included relative surface hydrophobicity by captive bubble contact angle, surface charge (i.e., degree of sulfonation) by uranyl cation binding, wt% solids, porosity, membrane thickness, water flux, and the affinity of membranes for a hydrophilic *Flavobacterium* and hydrophobic *Mycobacterium* species. The mycobacteria attached best to the MPS membranes, but the attachment of both organisms was inversely correlated with the mean aspect ratio of pores, suggesting that irregular or elliptical pores discouraged attachment. Multivariate regression analyses identified the pore mean aspect ratio, mean surface height, PS



content, and the n-methylpyrrolidone +propionic acid (NMP-PA) solvent concentration as influential factors in Mycobacterium attachment, whereas membrane thickness, surface roughness, pore mean aspect ratio, porosity, and the mean pore area/image area ratio influenced Flavobacterium attachment. Cluster analyses revealed that Mycobacterium attachment was associated with hydrophobic determinants of the MPS membranes, including PS content, wt% solids, and air bubble contact angle. In contrast, Flavobacterium attachment was primarily associated with membrane thickness and charge (i.e., uranyl cation binding or degree of sulfonation). Membrane flux was inversely correlated with surface hydrophobicity and PS content, but (in contrast to cell attachment) positively correlated with most pore geometry parameters including the mean aspect ratio, suggesting that pore geometry can be optimized to minimize cell attachment and maximize water transport. Other variables influencing water flux included the NMP-PA solvent concentration and membrane roughness. The results should facilitate the design of novel microporous PS membranes having reduced biofouling potentials and greater water fluxes. (C) 1999 Elsevier Science B.V. All rights reserved

- 40 Hall-Stoodley, L., Keevil, C.W., Lappin-Scott, H.M. (1999)
Mycobacterium fortuitum and Mycobacterium chelonae biofilm formation under high and low nutrient conditions
Journal of Applied Microbiology, 85, 60S-69S

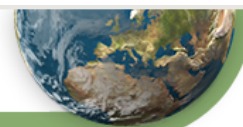
The rapidly growing mycobacteria (RGM) are broadly disbursed in the environment. They have been recovered from freshwater, seawater, wastewater and even potable water samples and are increasingly associated with non-tuberculous mycobacterial disease. There is scant evidence that nontuberculous mycobacteria (NTM) and RGM form biofilms. Therefore, an experimental system was designed to assess the ability of RGM to form biofilms under controlled laboratory conditions. A flat plate reactor flow cell was attached to either a high or low nutrient reservoir and monitored by image analysis over time. Two surfaces were chosen for assessment of biofilm growth: silastic which is commonly used in medical settings and high density polyethylene (HDPE) which is prevalent in water distribution systems. The results show that Mycobacterium fortuitum and M. chelonae formed biofilms under both high and low nutrient conditions on both surfaces studied. These results suggest that RGM may form biofilms under a variety of conditions in industrial and medical environments

- 41 Skuce, R.A., Brittain, D., Hughes, M.S., Neill, S.D. (1996)
Differentiation of Mycobacterium bovis isolates from animals by DNA typing
Journal of Clinical Microbiology, 34, 2469-2474

The insertion sequence IS6110 and the direct repeat (DR) specific to tuberculosis complex mycobacteria and the highly repeated DNA sequence, the polymorphic GC-rich repeat sequence (PGRS), were systematically used to identify restriction fragment length polymorphisms (RFLPs) within 210 isolates of Mycobacterium bovis. The isolates were primarily of bovine origin, but isolates from badgers, feral deer, sheep, humans, and a pig were included. The RFLP probes IS6110, DR, and PGRS individually identified 17, 18, and 18 different RFLP types, respectively, but in combination these probes identified a total of 39 different M. bovis RFLP types. The recommendations (J. D. A. van Embden, M. D. Cave, J. T. Crawford, J. W. Dale, K. D. Eisenach, B. Gicquel, P. W. M. Hermans, C. Martin, R. McAdam, T. M. Shinnick, and P. M. Small, J. Clin. Microbiol. 31:406-409, 1993) for a standardized RFLP analysis for M. tuberculosis were adapted to facilitate gel documentation, image analysis, and construction of a database of RFLP types. In the present study the same M. bovis RFLP types were evident in the various animal species included, indicating that the strains were not host restricted. Application of these techniques to defined field studies should help elucidate more accurately aspects of the epidemiology of bovine tuberculosis in different countries

- 42 Gelb, A.B., Venkateswaran, K.S., Vyas, G.N. (1996)
Editorial summary of the pre-symposium workshop on the Contemporary Assessment of Technologies
Biologicals, 24, 177-186

The following is the editor's summary of the Pre-symposium workshop on Contemporary Assessment of Technologies presented at the Symposium on Molecular Approaches to Laboratory Diagnosis at San Francisco in February 1995. This workshop was moderated by Dr Joel M. Palefsky, and Dr Michael P. Busch. We have briefly summarized the presentations by: (1) Dr Indira Hewlett of the Center for Biologics Evaluation and Research, Food and Drug Administration entitled 'Technology overview'; (2) Dr John J. Sninsky of Roche Molecular Systems Inc. entitled 'Polymerase Chain Reaction'; (3) Dr Terrance Walker of Becton Dickinson Research Center entitled 'Strand Displacement Amplification'; (4) Dr Mickey Urdea of Chiron Corporation entitled 'bDNA assay' and (5) Dr Robert H. Singer of University of Massachusetts Medical Center entitled 'Image analysis of in situ hybridization'. Although it was not possible to list all the references to the primary



literature, we have attempted to provide the key references as far as possible. (C) 1996 The International Association of Biological Standardization

- 43 Tanaka, S., Sato, M., Taniguchi, T., Yokomizo, Y. (1996)
Relationship of acid phosphatase activity to ultrastructural features in mice inoculated with Mycobacterium paratuberculosis
Journal of Comparative Pathology, 114, 81-91

Macrophage activation, measured as increased acid phosphatase (AcPase)-positive areas by image analysis, and ultrastructural features were examined in granulomatous mycobacterial lesions of mice innately susceptible (BALB/c mice; Bcg(s)) and innately resistant (C3H/HeJ mice; Bcg(r)) to Mycobacterium paratuberculosis strain ATCC 19698. In the liver and spleen of BALB/c mice 3 weeks after intraperitoneal inoculation with M. paratuberculosis, AcPase activity detected in epithelioid cell nodules was high; it had decreased, however, in the liver and spleen after a further 3 and 6 weeks, respectively. In C3H/HeJ mice, the size of epithelioid cell nodules in the liver and spleen was smaller than in BALB/c mice, and infiltrating macrophages, which had increased by week 9 after inoculation, showed high AcPase activity. Ultrastructurally, by week 32 in BALB/c mice, small phagolysosomes (SPLs) had greatly increased in number in the epithelioid cells. These SPLs contained a few AcPase-positive areas and a small number of bacteria, most of which were surrounded by an electron-translucent space (or electron-transparent zone [ETZ]). In contrast, only a few SPLs were observed in C3H/HeJ mice at week 32; in the liver and spleen, large phagolysosomes (LPLs) showed high AcPase activity and contained many degenerated bacteria, which also had an ETZ. These results suggest that the enzymatic and ultrastructural differences in phagolysosomes between BALB/c mice and C3H/HeJ mice reflect the susceptibility of these mouse strains to M. paratuberculosis. (C) 1996 W.B. Saunders Company Limited

- 44 Skuce, R.A., Brittain, D., Hughes, M.S., Beck, L.A., Neill, S.D. (1994)
Genomic Fingerprinting of Mycobacterium-Bovis from Cattle by Restriction-Fragment-Length-Polymorphism Analysis
Journal of Clinical Microbiology, 32, 2387-2392

Two insertion sequences, IS6110 and IS1081, specific to the tuberculosis complex mycobacteria and a highly reiterated DNA element (pTBN12) cloned from Mycobacterium tuberculosis were systematically used to identify restriction fragment length polymorphism (RFLP) types among bovine isolates of Mycobacterium bovis in Northern Ireland. In a sample of 109 isolates, probes IS6110, IS1081, and pTBN12 identified 10, 2, and 12 distinct patterns, respectively. By combining the patterns generated by the three probes it was possible to identify 28 distinct RFLP types. The standard protocol advocated for RFLP analysis of M. tuberculosis was used and would facilitate computer-based gel documentation and image analysis to establish a database of M. bovis types for large-scale epidemiological studies. These procedures will facilitate interlaboratory comparisons of M. bovis isolates and will help to elucidate the precise epidemiology of bovine tuberculosis in different countries

- 45 Orrell, J.M., Brett, S.J., Ivanyi, J., Coghill, G., Grant, A., Beck, J.S. (1992)
Measurement of the Immunoperoxidase Staining of Macrophages Within Liver Granulomata of Mice Infected with Mycobacterium-Tuberculosis
Analytical and Quantitative Cytology and Histology, 14, 451-458

A quantitative image analysis technique developed for the measurement of the extent of macrophage activation and epithelioid cell differentiation was performed on mice infected experimentally with Mycobacterium tuberculosis. The granulomatous inflammatory response within the liver reached a peak at day 23 and declined by day 33. Animals of strain B10.BR (H-2k) showed an increased granuloma fraction as compared to Balb/k (H-2k) mice, thus confirming the influence of non-H2 genes in the control of granuloma formation in mice. Using a monoclonal antibody against CD11b/CD18 (Mac1;CR3), we observed two subpopulations of macrophages within the granulomata. The small, darkly staining cells at the periphery of granulomata appear to be newly recruited macrophages. Larger, paler staining cells toward the center of granulomata represent activated and mature epithelioid macrophages. Using a semiautomated image analyzer (Quantimet 970), we measured the relative numbers of these macrophage subpopulations. There were more activated macrophages (epithelioid cells) associated with the increased granuloma fraction in the B10.BR mice than in the Balb/k. However, similar numbers of newly recruited peripheral macrophages were found in both Balb/k and B10.BR strains. This technique has shown qualitative as well as quantitative differences in the granulomatous inflammatory response in this murine model of tuberculosis in strains of mice with quite different antibody repertoires to mycobacterial antigens